DEVELOPMENT OF COST-EFFECTIVE SURFACTANT FLOODING TECHNOLOGY

Quarterly Report for the Period
July 1995 – September 1995

By
Gary A. Pope
Texaco Centennial Chair in Petroleum Engineering

Kamy Sepehrnoori
Frank W. Jessen Professor in Petroleum Engineering

Work Performed under Contract No. DE–AC22–92BC14885

Nancy Toppetta, Contract Administrator
U.S. Department of Energy
Pittsburgh Energy Technology Center
P.O. Box 10940, MS 921-118
Pittsburgh, PA 15236-0940

Prepared by
The University of Texas
Center for Petroleum and Geosystems Engineering
Department of Petroleum Engineering
Austin, TX 78712

OBJECTIVES

The objective of this research is to develop cost-effective surfactant flooding technology by using surfactant simulation studies to evaluate and optimize alternative design strategies taking into account reservoir characteristics, process chemistry, and process design options such as horizontal wells. Task 1 is the development of an improved numerical method for our simulator that will enable us to solve a wider class of these difficult simulation problems accurately and affordably. Task 2 is the application of this simulator to the optimization of surfactant flooding to reduce its risk and cost.

SUMMARY

The objective of Task 2 is to investigate and evaluate, through a systematic simulation study, surfactant flooding processes that are cost-effective. We previously have reported on low tension polymer flooding as an alternative to classical surfactant/polymer flooding. In this reporting period, we have studied the potential of improving the efficiency of surfactant/polymer flooding by coinjecting an alkali agent such as sodium carbonate under realistic reservoir conditions and process behavior. The alkaline/surfactant/polymer (ASP) flood attempts to take advantage of high pH fluids to reduce the amount of surfactant needed by the chemical reactions between injection fluid and formation fluid or formation rocks. The main mechanisms included in ASP flood and are modeled in UTCHEM are the following:

reduction of surfactant adsorption,
chemical reactions,
phase behavior of surfactant,
in situ generated surfactant, and
cation exchange with clay and surfactant.

We performed for the first time mechanistic field-scale ASP simulations in three dimensions. An areal view of the grid and the location of 13 wells (four injectors and 9 producers) is shown in Fig. 1. The permeability field was generated stochastically based on a log normal distribution and conditioned for the well data (Table 1). The permeability distribution in the top layer of the reservoir is shown in Fig. 2. The correlation lengths in the x, y, and z directions were 184.8m, 184.8 m, and 2 m, respectively. The top layer initial oil saturation and porosity contours are shown in Fig. 3. The 0.51 PV ASP slug consisted of 1.8 wt% sodium carbonate as the alkali agent, 0.15 wt% polymer and 0.002 volume fraction surfactant. The chemical slug was followed by 0.26 PV of 0.15 wt% polymer drive followed by formation water (Table 2). The injected pH was 11.

Based on the water analysis shown in Table 3, seven elements, eighteen fluid species, four solid species, four clay-adsorbed cations, and three surfactant-adsorbed cations were considered in chemical reactions. The elements chosen in this study were hydrogen, sodium, calcium, magnesium, carbonate, chloride, and acid (from HA). The acid number of the crude oil was 1.96. The chemical reactions can be classified into five categories: oil-alkali chemical reactions, homogeneous aqueous reactions, dissolution and precipitation reactions, ion exchange with clay minerals, and ion exchange with micelles. The homogeneous aqueous reactions include various dissociation reactions of the weak acids and bases. Table 4 lists the elements, species, chemical reactions and equilibrium constants used in this study.

Figure 4 shows a comparison of the cumulative oil recovery for ASP, alkaline/polymer (AP), polymer flooding and water flooding. The oil recovery results are also given in Table 2. The oil saturation profile at the end of the ASP flood indicates a significant recovery of the oil phase inside the well pattern.

DEVELOPMENT OF COST-EFFECTIVE SURFACTANT FLOODING TECHNOLOGY

Contract No. DE–AC22–92BC14885

The University of Texas
Austin, TX

Contract Date: September 30, 1992
Anticipated Completion: December 31, 1995
Government Award: $765,557 (Total funding)

Principal Investigators:
Gary A. Pope
Kamy Sepehrnoori

Contracting Officer Representative:
Nancy Toppetta
Pittsburgh Energy Technology Center

Reporting Period: July 1, 1995 – September 30, 1995

Table 1. Statistical data for the permeability field

Variable	λ_x / λ_z	Arithmetic Mean
Permeability, md		
Layer1	92.4	164.3
Layer2		133.8
Layer3		150.3
Layer4		74.07
Layer5		53.92

Correlation length in x and y directions $\lambda_x = \lambda_y = 184.8$ m;
Seed number = 87654, Log normal distribution

Table 2. Summary of simulation data

Flood	Injection Scheme	Injection Concentration			Amount of chemical (tons)		
	Slug size, PV	Surfactant (vol. frac.)	Polymer (wt%)	Na_2CO_3 (wt%)	Surfactant	Polymer	Oil recovery (%ROIP)
Alkaline/Surf./Polymer	0.51 ASP 0.26 P 0.70 W	0.002	0.15 0.15	1.8	76.5	87.21	17
Alkaline/Polymer	0.51 AP 0.26 P 0.70 W	-------	0.15 0.15	1.8	None	87.21	13
Polymer	0.76 P 0.70 W	-------	0.15	-------	None	87.21	8.0
Water	1.46 W	-------	-------	-------	None	None	2.5

Remaining oil in place (ROIP)= 30,158 m^3

Table 3. Summary of water analysis for makeup water and formation water used in the field scale simulations

Name of Ions	Formation water (meq/ml)	Makeup water (meq/ml)
Na^{+}	0.1043	0.0023
Mg^{2+}	0.003	0.00095
Ca^{2+}	0.00271	0.00336
Cl^{-}	0.05892	0.00109
HCO_3^{-}	0.04301	0.0025
CO_3^{2-}	0.008	0.002
SO_4^{2-}	-------	0.0028

Table 4. List of elements, reactive species, and reactions

Elements or pseudo-element:	Hydrogen (reactive), Sodium, Calcium, Magnesium, Carbonate, A (from acid HA), Chlorine
Independent aqueous or oleic species:	H^{+}, Na^{+}, Ca^{2+}, Mg^{2+}, CO_3^{2-}, HA_o, Cl^{-}, H_2O
Dependent aqueous or oleic species:	$Ca(OH)^{+}$, $Mg(OH)^{+}$, $Ca(HCO_3)^{+}$, HA_w, $Mg(HCO_3)^{+}$, OH^{-}, HCO_3^{-}, A^{-}, H_2CO_3, $CaCO_3^{o}$, $MgCO_3^{o}$
Solid species:	$CaCO_3$ (Calcite), $Ca(OH)_2$ (Calcium hydroxide), $MgCO_3$ (Magnesite), $Mg(OH)_2$ (Magnesium hydroxide)
Adsorbed cations:	$\overline{H}^{+}$, $\overline{Na}^{+}$, $\overline{Ca}^{2+}$, $\overline{Mg}^{2+}$
Adsorbed cations on micelles:	$\overline{\overline{Na}}^{+}$, $\overline{\overline{Ca}}^{2+}$, $\overline{\overline{Mg}}^{2+}$

Table 4. (Cont.)

Aqueous reactions	Equilibrium constant
$H_2O \overset{K_1^{eq}}{\rightleftarrows} H^+ + OH^-$	$K_1^{eq} = [H^+][OH^-]$
$HA_w + OH^- \overset{K_2^{eq}}{\rightleftarrows} A^- + H_2O$	$K_2^{eq} = \frac{[A^-][H^+]}{[HA_w]}$
$H^+ + CO_3^{2-} \overset{K_3^{eq}}{\rightleftarrows} HCO_3^-$	$K_3^{eq} = \frac{[HCO_3^-]}{[H^+][CO_3^{2-}]}$
$Ca^{2+} + H_2O \overset{K_4^{eq}}{\rightleftarrows} Ca(OH)^+ + H^+$	$K_4^{eq} = \frac{[Ca(OH)^+][H^+]}{[Ca^{2+}]}$
$Mg^{2+} + H_2O \overset{K_5^{eq}}{\rightleftarrows} Mg(OH)^+ + H^+$	$K_5^{eq} = \frac{[Mg(OH)^+][H^+]}{[Mg^{2+}]}$
$Ca^{2+} + H^+ + CO_3^{2-} \overset{K_6^{eq}}{\rightleftarrows} Ca(HCO_3)^+$	$K_6^{eq} = \frac{[Ca(HCO_3)^+]}{[Ca^{2+}][CO_3^{2-}][H^+]}$
$Mg^{2+} + H^+ + CO_3^{2-} \overset{K_7^{eq}}{\rightleftarrows} Mg(HCO_3)^+$	$K_7^{eq} = \frac{[Mg(HCO_3)^+]}{[Mg^{2+}][CO_3^{2-}][H^+]}$
$2H^+ + CO_3^{2-} \overset{K_8^{eq}}{\rightleftarrows} H_2CO_3$	$K_8^{eq} = \frac{[H_2CO_3]}{[CO_3^{2-}][H^+]^2}$
$Ca^{2+} + CO_3^{2-} \overset{K_9^{eq}}{\rightleftarrows} CaCO_3^o$	$K_9^{eq} = \frac{[CaCO_3^o]}{[Ca^{2+}][CO_3^{2-}]}$
$Mg^{2+} + CO_3^{2-} \overset{K_{10}^{eq}}{\rightleftarrows} MgCO_3^o$	$K_{10}^{eq} = \frac{[MgCO_3^o]}{[Mg^{2+}][CO_3^{2-}]}$

Partitioning of HA	Partition coefficient
$HA_o \overset{K_D}{\rightleftarrows} HA_w$	$K_D = \frac{[HA_w]_{water}}{[HA_o]_{oil}}$

Table 4. (Cont.)

Dissolution reactions	Solubility product
$CaCO_3 \overset{K_1^{sp}}{\rightleftarrows} Ca^{2+} + CO_3^{2-}$	$K_1^{sp} = [Ca^{2+}]\,[CO_3^{2-}]$
$MgCO_3 \overset{K_2^{sp}}{\rightleftarrows} Mg^{2+} + CO_3^{2-}$	$K_2^{sp} = [Mg^{2+}]\,[CO_3^{2-}]$
$Ca(OH)_2 \overset{K_3^{sp}}{\rightleftarrows} Ca^{2+} + 2OH^-$	$K_3^{sp} = [Ca^{2+}][H^+]^{-2}$
$Mg(OH)_2 \overset{K_4^{sp}}{\rightleftarrows} Mg^{2+} + 2OH^-$	$K_4^{sp} = [Mg^{2+}][H^+]^{-2}$
Exchange reactions (on matrix)	**Exchange equilibrium constant**
$2\overline{Na}^+ + Ca^{2+} \overset{K_1^{ex}}{\rightleftarrows} 2Na^+ + \overline{Ca}^{2+}$	$K_1^{ex} = \dfrac{[\overline{Ca}^{2+}]\,[Na^+]^2}{[Ca^{2+}]\,[\overline{Na}^+]^2}$
$2\overline{Na}^+ + Mg^{2+} \overset{K_2^{ex}}{\rightleftarrows} 2Na^+ + \overline{Mg}^{2+}$	$K_2^{ex} = \dfrac{[\overline{Mg}^{2+}]\,[Na^+]^2}{[Mg^{2+}]\,[\overline{Na}^+]^2}$
$\overline{H}^+ + Na^+ + OH^- \overset{K_3^{ex}}{\rightleftarrows} \overline{Na}^+ + H_2O$	$K_3^{ex} = \dfrac{[Na^+]\,[\overline{H}^+]}{[\overline{Na}^+]\,[H^+]}$
Exchange reactions (on micelle)	**Exchange equilibrium constant**
$2\bar{\bar{Na}}^+ + Ca^{2+} \overset{K_1^{exm}}{\rightleftarrows} 2Na^+ + \bar{\bar{Ca}}^{2+}$	$K_1^{exm} = \dfrac{[\bar{\bar{Ca}}^{2+}]\,[Na^+]^2}{[\bar{\bar{Na}}^+]^2\,[Ca^{2+}]}$ where $K_1^{exm} = \beta_1^{exm}\{[A^-] + [S^-]\}$
$2\bar{\bar{Na}}^+ + Mg^{2+} \overset{K_2^{exm}}{\rightleftarrows} 2Na^+ + \bar{\bar{Mg}}^{2+}$	$K_2^{exm} = \dfrac{[\bar{\bar{Mg}}^{2+}]\,[Na^+]^2}{[\bar{\bar{Na}}^+]^2\,[Mg^{2+}]}$ where $K_2^{exm} = \beta_2^{exm}\{[A^-] + [S^-]\}$

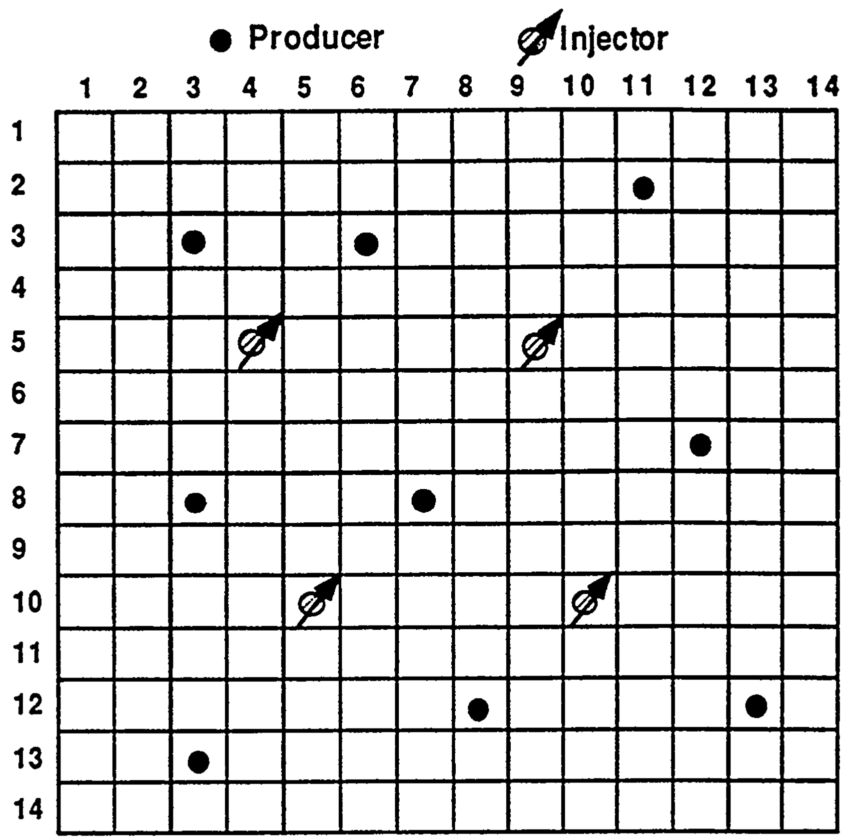

Fig.1. Schematic of well pattern and grid used in the ASP simulations

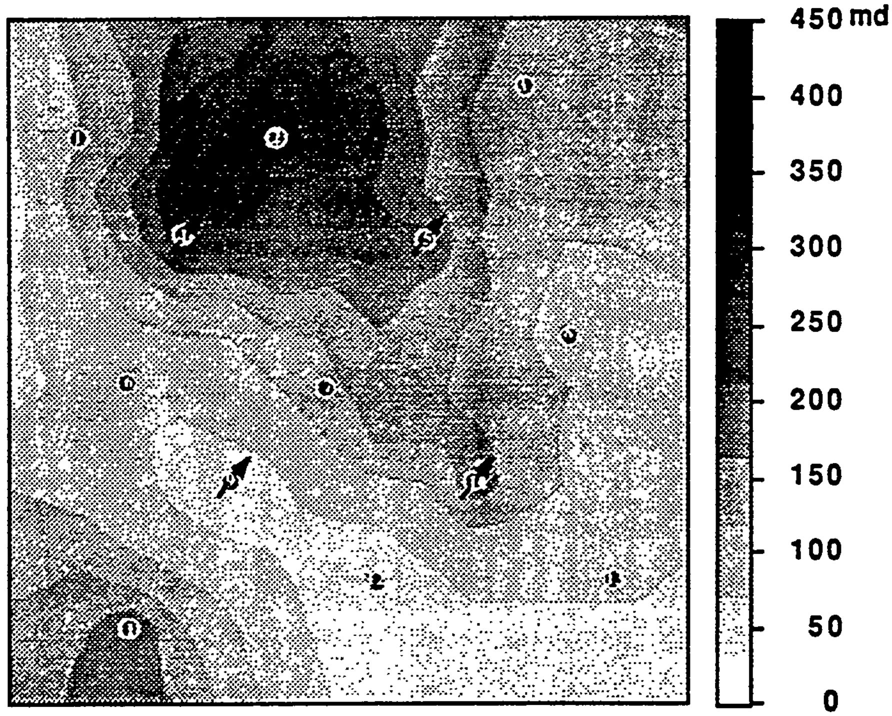

Fig. 2. Permeability field in layer 1

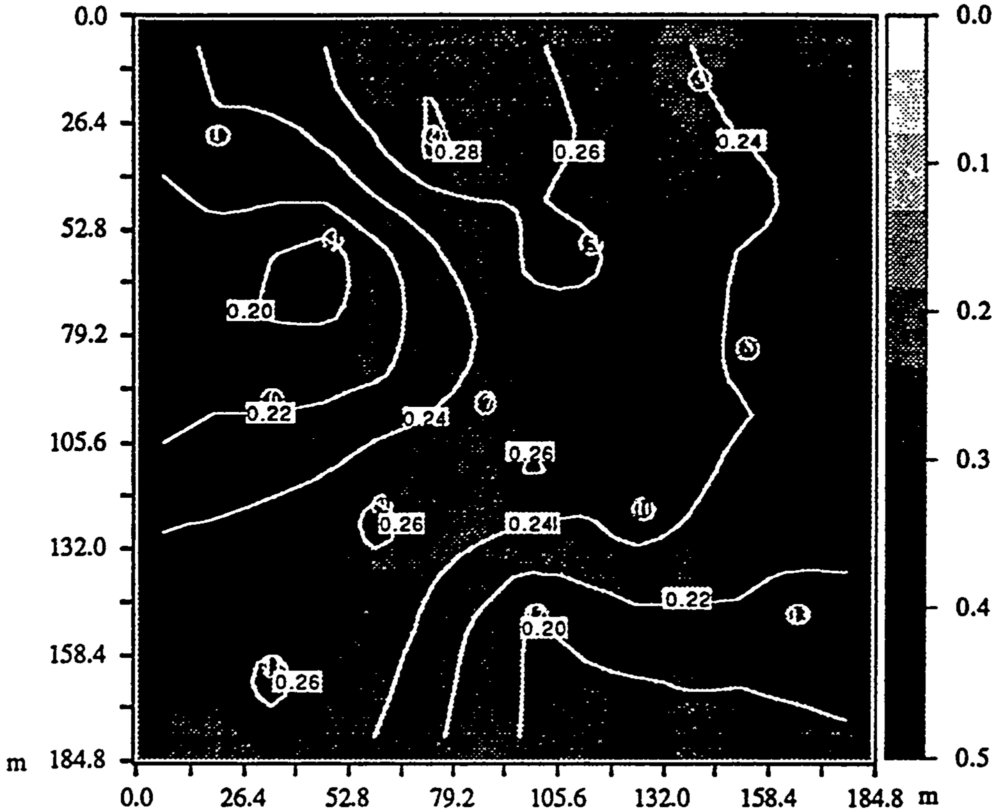

Fig. 3. Initial oil saturation overlaid by porosity contour for layer 1

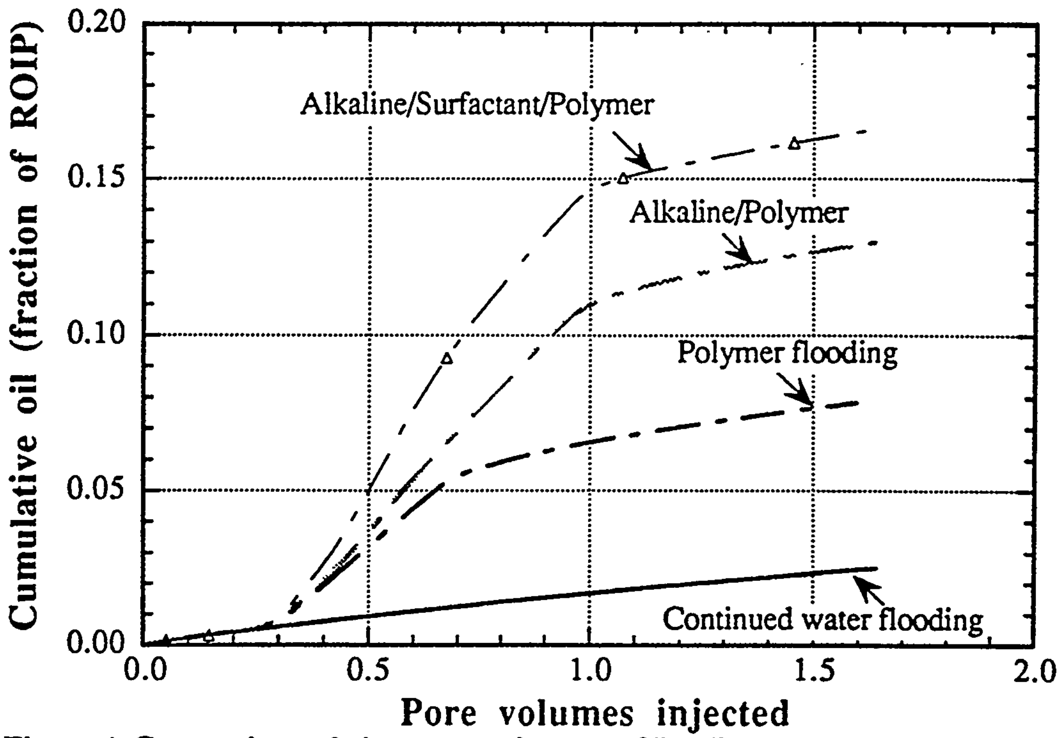

Figure 4. Comparison of oil recovery for the ASP, AP, polymer, and water flood